



International journal of basic and applied research

www.pragatipublication.com

ISSN 2249-3352 (P) 2278-0505 (E)

Cosmos Impact Factor-5.86

Energy Management of Hybrid Grid Connected Power Systems with NN Controller

Badavath Srikanth¹, K. Ranjith Kumar²

1, PG Student, Department of Electrical and Electronics Engineering

2, Associate Professor, Department of Electrical and Electronics Engineering

Vaagdevi College of Engineering, Bollikunta, Warangal (Dt), TS, India.

Srikanthbadavath4951@gmail.com

Abstract: Renewable energy sources are being more relied upon to provide power as a result of increasing energy prices, grid losses, concerns about nuclear power, and other global environmental developments. Smart towns and colleges, which use smart grid technology, are becoming increasingly popular places to live and work for many people. Energy management is made more difficult by the fact that these smart grid systems rely heavily on hybrid energy sources. Consequently, it is critical to develop an intelligent controller for energy management. In order to regulate a smart DC-microgrid, this study suggests a sophisticated intelligent energy management controller that combines fuzzy logic, ANN, and fractional-order proportional-integral-derivative (FO-PID) techniques. The DC-microgrid incorporates a battery bank, wind power, and photovoltaic (PV) power as its hybrid energy sources. In order to maximise power extraction from wind and PV while enhancing power quality, the source-side converters (SSCs) are controlled using a new intelligent fractional-order PID approach that is enhanced with an ANN controller. Wind and PV power gets top billing in order of affordability. By inserting the ANN controller into the system, throughput is further enhanced, contributing to higher power quality, greater consistency in output, and enhanced service continuity. The suggested control schema outperforms previous approaches, including the super twisting fractional-order controller, as demonstrated by Matlab/Simulink simulation results, particularly when using the ANN controller

Keywords Microgrid, Fuzzy, PMSG, MPPT, Battery Bank

1.0 Introduction

There are a lot of obstacles in the way of progress and growth for electrical power systems. These are now environmental and social in nature, rather than only technical, economic, or financial. Major threats to 21st century energy and environmental security include climate change and sustainable development. Traditional energy sources have polluting effects on the



environment and drive up the price of generating electricity. The environment is being negatively impacted by the rapid expansion of energy demand, and these effects will persist for quite some time. These challenges may be surmounted with the use of renewable energy sources including wind power, solar photovoltaics, and tidal power.

Solar irradiance, temperature, and wind speed are just a few examples of the varying climatic conditions that exist across the globe. It may be the reason why solar panels and wind turbines aren't producing enough electricity. The concept of Hybrid Energy Systems (HES) has been presented to effectively and affordably use the renewable energy resources. In this project, we build power management and control systems, as well as test and validate the corresponding algorithms in a simulated environment. The model of a solar photovoltaic, wind, or diesel energy conversion system must be developed and simulated using mathematical modelling.

A cutting-edge power grid makes use of cutting-edge technologies to boost efficiency, dependability, and adaptability. Microgrids are set to become the most significant future driver of change in the electric power infrastructure due to a confluence of technical, economic, and social considerations. In many areas, the price of distributed generation may now compete with that of power from the grid. Clean natural gas fueled and diesel production, for instance, is cheap due to very low gas costs, while the price of photovoltaic (PV) panels and inverters continues to fall. The importance of incorporating renewable energy sources has been recognised as a possible long-term solution.

All throughout the world, people are beginning to see that standalone hybrid solar-wind power generation systems are a better option than either connecting to the grid or using traditional fossil fuels to power outlying areas. The 2006 Statistics Canada Census estimated a population of 194,281 in Canada's 292 off-grid remote settlements. These places have enormous potential for harnessing wind power. The majority of the fossil fuel used to generate electricity is diesel, and the annual demand is at 1,477,415 MWh. Due to the high cost and carbon pollution caused by running diesel generators, a new approach is needed to reduce diesel use. Solar photovoltaic electricity in Canada increased at an annual rate of 147.3% between 2008 and 2011. Furthermore, wind power generation has become increasingly popular, and by 2020, it is expected to generate 12% of the world's electricity. As a result, researchers in the electrical



power business are starting to pay more attention to the concept of hybrid operation. Gaspé, Quebec is home to the hybrid renewable energy operation established by TechnoCentre Éolien (TCÉ). The primary goal of this research is to analyse the functionality and usefulness of a hybrid energy system that can function independently.

2.0 Suggested Microgrid System

The microgrid system being studied comprises a Photovoltaic (PV) system, a WECS-PMSG (Wind Energy Conversion System based Permanent Magnet Synchronous Generator), and various power electronic devices. Each high-powered electrical appliance within the microgrid requires multiple controllers. Figure 1 illustrates the proposed setup and schematic diagram of the microgrid system. The following subsections will provide a detailed overview of the configuration of each component.

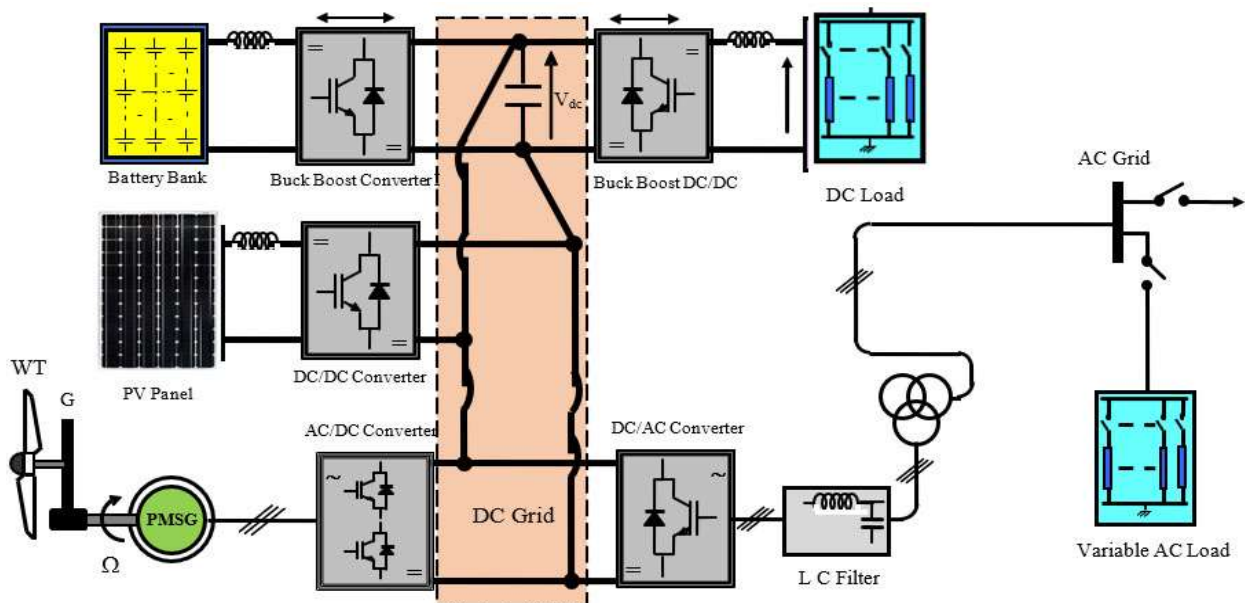


Fig.1 Test system structure.

2.1 PV system

The voltage–current (V-I) characteristics of the used PV model are given by [16]:

$$I_{pv} = I_{ph} - I_s e^{\left(\frac{q(V_{pv} + R_s I_{pv})}{nkT} - 1\right)} - \frac{V_{pv} + R_s I_{pv}}{R_{sh}}$$

where I_{ph} is the photocurrent, I_s is the diode saturation current, q is the electron charge, T is the temperature in Kelvin (K), n is the P-N junction ideality factor, and R_s and R_{sh} are the



intrinsic series and shunt resistances of the PV cell. The PV model is depicted in Figure 2 as a schematic.

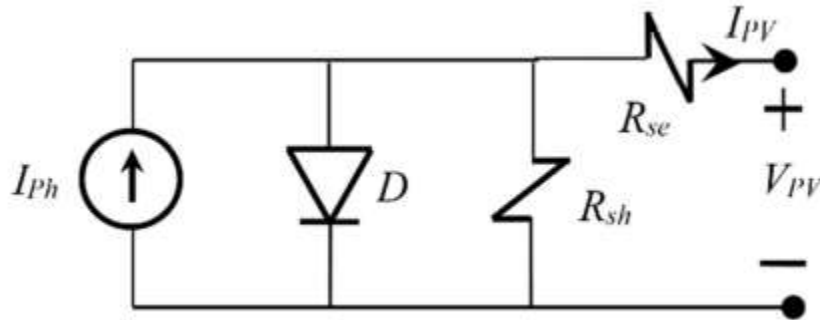


Fig 2. Equivalent circuit of a PV cell

Three series and six parallel strings make up the linked PV system, which generates 3.84 kW at 1000 W/m² full irradiance. Solar photovoltaic (PV) modules' voltage-current and voltage-power relationships are shown in Figure 3. As can be seen in this graph, the PV panel's open circuit voltage is where the highest power is produced. Under Standard Test Conditions, this panel is rated at 215 W. The highest power voltage is 29 volts, and the open circuit voltage is 36.6 volts. 7.84 A and 7.35 A are the short circuit and peak currents, respectively. Additional details and technical specs for this panel can be found in [17,18].

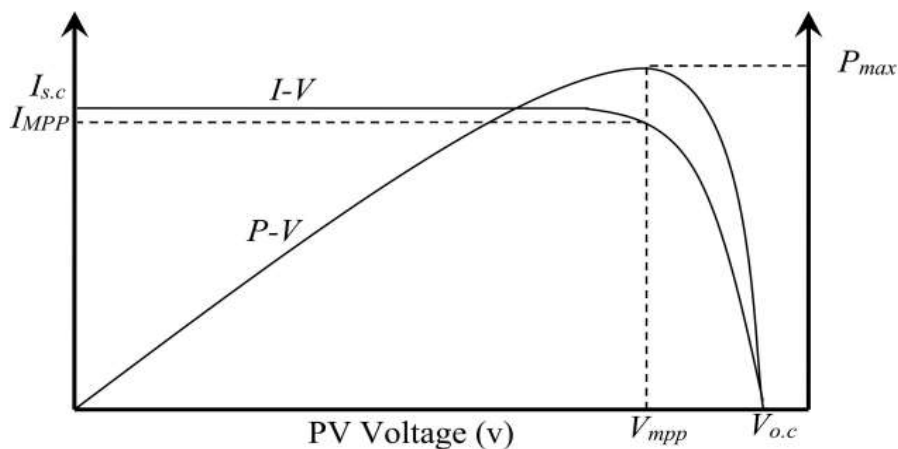


Fig 3. Characteristics of PV cells

2.2. WECS

Wind turbines play a vital role in wind energy systems, serving as the primary movers by coupling electric generators to their shafts. These turbines come in two main varieties:



horizontal axis and vertical axis. Horizontal axis turbines rotate in one direction, while vertical axis turbines rotate in the opposite direction. Additionally, wind turbines can be categorized based on their operating speed into constant and variable types.

The mode of operation of a Wind Energy Conversion System (WECS) is primarily determined by the characteristics of the wind turbine and the type of wind generator used. These factors dictate how efficiently the system can harness wind energy to generate electricity.

2.2.1. Wind Turbine Characteristics

The output power generated by the wind turbine can be given in terms of the turbine aerodynamic power coefficient (C_p), as follows [18,19]:

$$P = 0.5 \rho_a A C_p v^3$$

The aerodynamic power coefficient of a wind turbine is a performance indicator, which is influenced by the blade pitch angle (β) and the tip-speed ratio (λ). A generic equation of C_p based on the turbine characteristics is given by (2) [20–22]:

$$C_p(\lambda, \beta) = C_1 \left(\frac{C_3}{\lambda_i} - C_3 \beta - C_4 \right) e^{-\frac{C_5}{\lambda_i}} + C_6 \lambda$$

where the coefficients C_1 to C_6 are: $C_1 = 0.5176$, $C_2 = 116$, $C_3 = 0.4$, $C_4 = 5$, $C_5 = 21$, and $C_6 = 0.0068$, and

$$\lambda = \frac{\omega R}{V_w}$$
$$\frac{1}{\lambda_i} = \frac{1}{\lambda + 0.08\beta} - \frac{0.035}{\beta^3 + 1}$$

R is the turbine radius in (m), V_w is the wind speed in (m/s), and ω is the turbine angular speed in (rad/s). Figure 4 shows power characteristics of a typical wind turbine with $\beta =$ zero and variable speed operation [20-22].

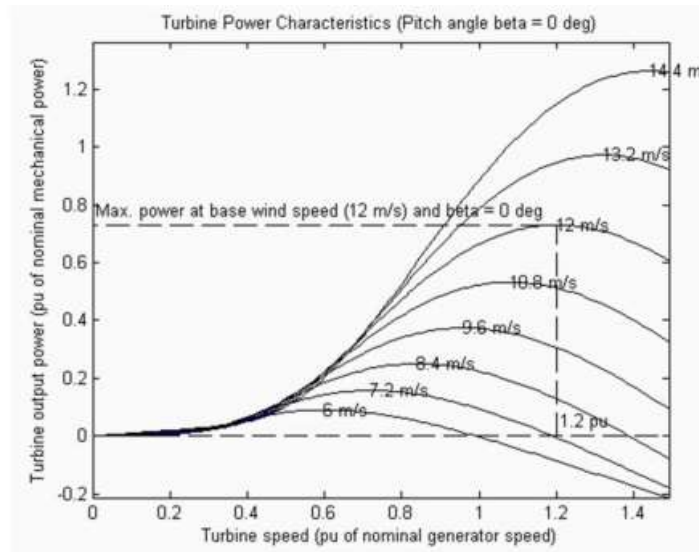


Fig 4. Power characteristics of a typical wind turbine

2.2.2. Permanent Magnet Synchronous Generators

In a Wind Energy Conversion System (WECS), the Permanent Magnet Synchronous Generator (PMSG) is commonly designed with multiple poles, allowing it to operate efficiently at low speeds synchronized with the rotational speed of the wind turbine. This direct-drive configuration, often referred to as a direct-drive system, eliminates the need for gearboxes, unlike systems based on Doubly Fed Induction Generators (DFIG) which require them. This absence of gearboxes reduces installation and maintenance costs, providing a cost-saving advantage.

The PMSG is capable of operating across a wide range of rotor speeds, making it suitable for variable-speed applications. The output voltage generated at the stator terminals of a PMSG varies in frequency and amplitude in response to changes in wind speed. To connect the stator to the grid, a power electronic converter is required. Figure 6 illustrates a typical configuration of a PMSG-based wind energy conversion system.

One notable advantage of the PMSG-based system is that it operates without additional rotor control. This means that the power converters used can be rated at full capacity, enabling efficient conversion of wind energy across a broad range of wind speeds. Moreover, power converters operating at full capacity facilitate compliance with various grid regulations and require no additional hardware for fault ride-through situations.

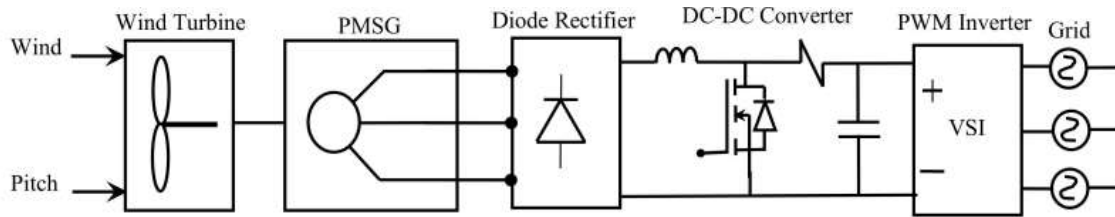


Fig 5. Typical PMSG based wind energy conversion system.

2.3 Bidirectional DC–DC Converter with a Battery Storage System

In most photovoltaic (PV) systems, lead-acid batteries are commonly employed for energy storage. To manage the charging and discharging of these batteries, bidirectional DC-DC converters are utilized. Various topologies and configurations of bidirectional DC-DC converters have been explored in prior research [15,16]. However, in this study, a buck-boost DC-DC converter is adopted for the charging and discharging processes.

Fig.6 illustrates the typical setup of the bidirectional converter utilized in this paper. The converter operates as a buck converter when the PV output is high, with the gate signal provided to the switch S1. This mode is engaged to charge the batteries efficiently. Conversely, when the power from the PV system is low or the grid is unavailable, the bidirectional converter functions as a boost converter. In this scenario, the gate signal triggers switch S2, causing the battery to discharge and supply power to the load.

The parameters of the bidirectional converter are determined by equations (13) through (15), ensuring optimal operation and efficiency in both charging and discharging modes.

$$C_H = \frac{D}{R_H f_s (\Delta V_H / V_H)}$$
$$L_{b, \min} \geq \frac{D(1-D)^2 R_H}{2f_s}$$

where R_L and R_H are the load resistance at buck and boost sides, respectively. C_H is the capacitance value at the boost side. $L_{b, \min}$ is the minimum value of the inductance and f_s is the switching frequency. Other specifications of this microgrid are shown in Table 1.

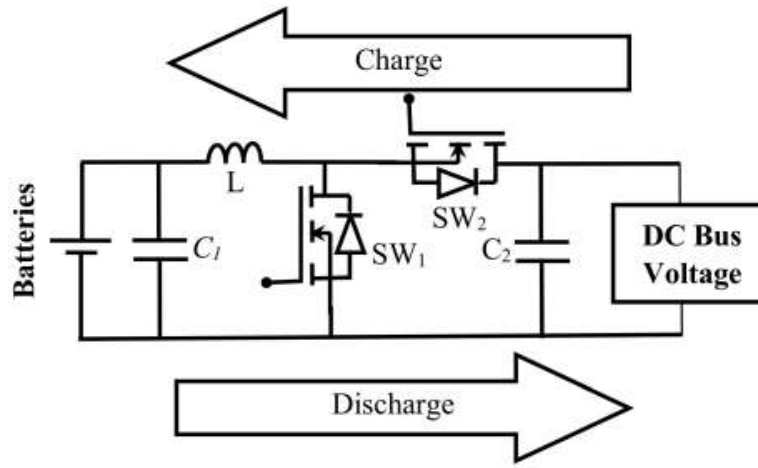


Fig 6 Bidirectional buck–boost converter.

Table 1. Sizing and specifications of the microgrid system.

Load Sizing	DC Bus Voltage	700 Vdc
	Load Power Required	2 kW
Battery Sizing	Batteries capacity	102 Ah
	Battery Voltage	96 Vdc
	Batteries capacity	9.8 kWh
	Batteries strings (parallel)	1
	Batteries per string (series)	4
PV Array Sizing	PV module	Soltech 1STH-215-P
	Max power per module	213 W
	Max current	7.35 A
	Max voltage	29 V
	Parallel Strings	6
	Series Modules per string	3
PMSG	Rated Power	3 kW
	Rated Speed	360 RPM

2.4 ANN controller

An Artificial Neural Network (ANN)-based controller for a grid-integrated hybrid microgrid is designed to manage and optimize the operation of multiple power sources (e.g., solar panels, wind turbines) and energy storage systems within a microgrid environment. The ANN-based controller leverages machine learning algorithms to analyze complex patterns in power demand, renewable energy generation, and grid conditions in real time.



The primary goal of this controller is to enhance energy efficiency, maintain power quality, and ensure the stability of the microgrid when integrated with the main power grid. It can predict power fluctuations, balance the supply and demand of energy, and make quick adjustments based on learned historical data and current operating conditions.

ANN-based controllers excel in adapting to variable conditions, such as fluctuations in solar irradiance, wind speeds, and load changes, by continuously learning and updating their operational strategies. This adaptive quality makes ANN-based controllers ideal for hybrid microgrids, where multiple power sources need to operate seamlessly in conjunction with each other and with the main power grid. Additionally, they are effective in handling uncertainties and non-linear behaviors, leading to enhanced reliability and resilience in microgrid operations.

3 Simulation Outcomes

The simulation results and settings utilized for the proposed system can be found in [29]. The voltage of the DC link is consistently maintained at 240 V. This simulation study focuses on evaluating the performance of an energy management system.

Initially, the battery storage system connects an 8000-watt DC load to the DC-link, starting with an initial state of charge (SOC) of 80%. This connection is facilitated by two load-side converters.

Fig. 8 illustrates the wind profile, showcasing wind speeds ranging from 8 to 13 m/s. Meanwhile, Figure 14 provides insight into the range of wind power, varying between 4000 and 10000 watts depending on wind speed.

Under conditions of 25 degrees Celsius and a brightness of 600 watts per square meter, a photovoltaic (PV) array is capable of producing 3000 watts of power, as depicted in Figure 10.

The combined output of solar and wind energy, denoted as P_{dg} , is presented in Figure 11. The data indicates that P_{dg} generates power within the range of 7000 to 13000 watts.

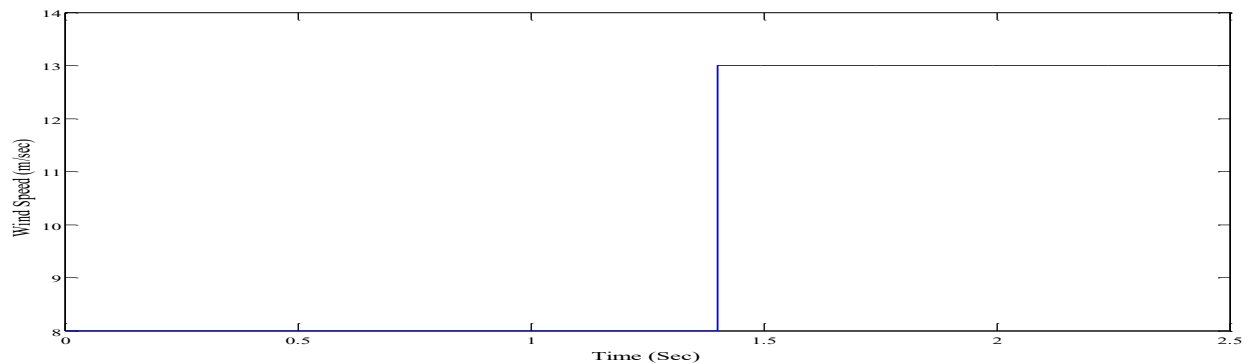


Fig 8. Wind Speed

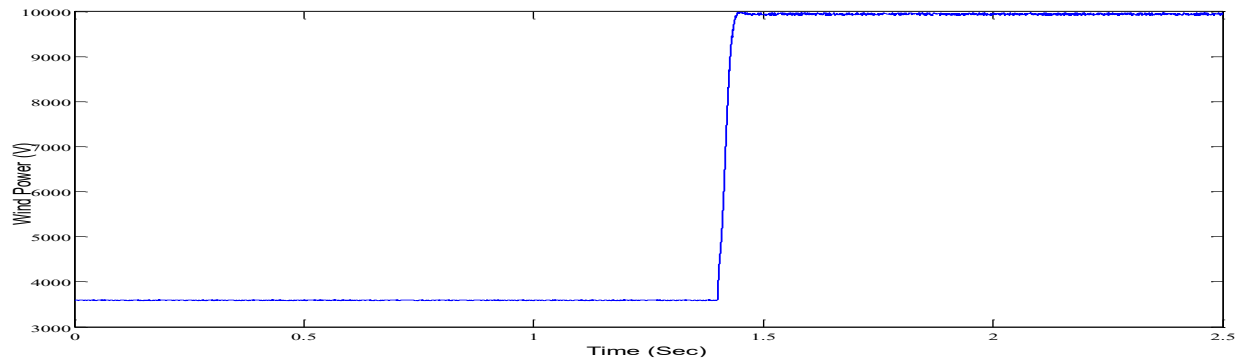


Fig.9 Wind Power

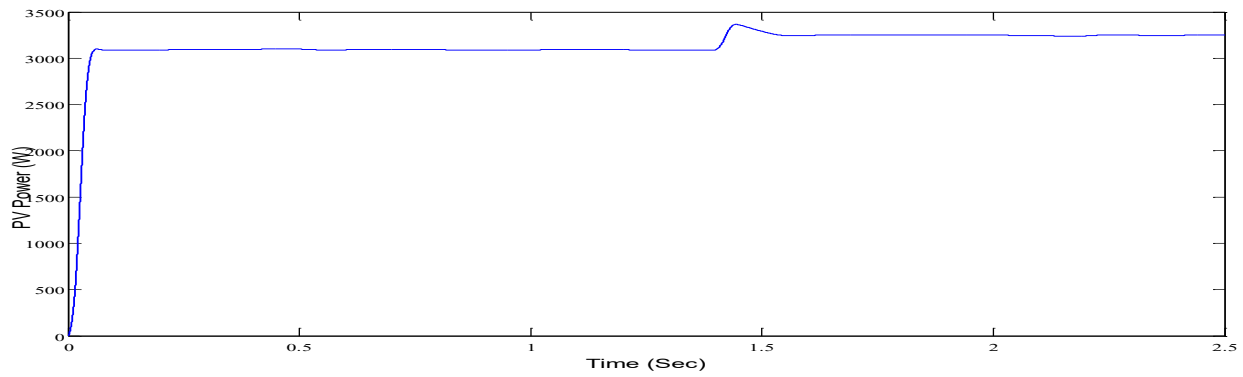


Fig.10 PV Power

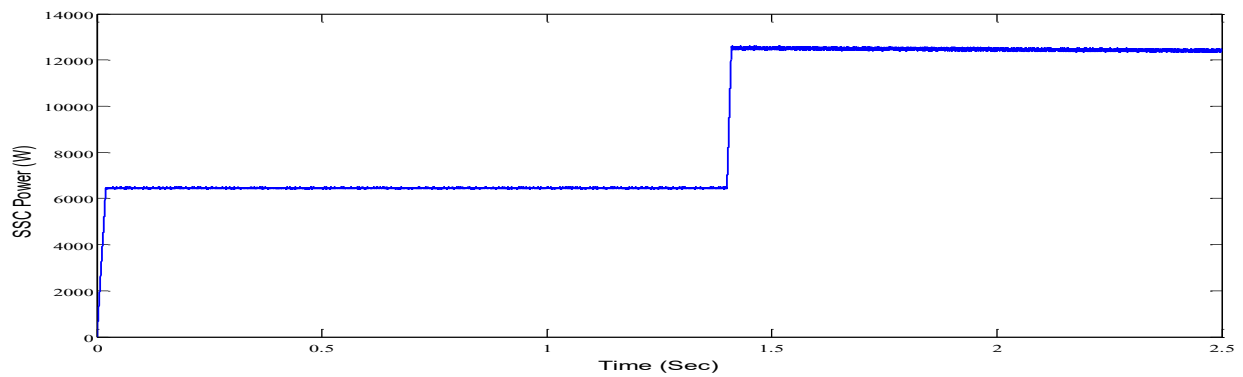


Fig.11 SSCs Power

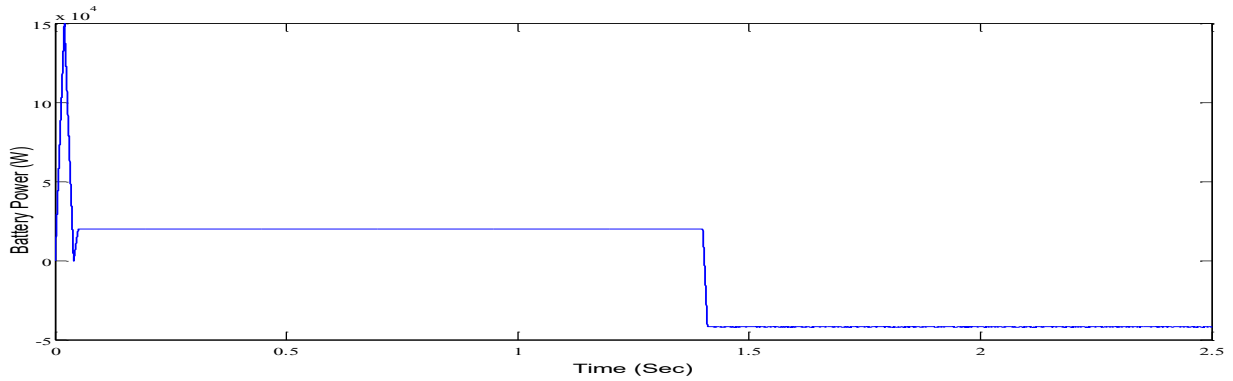


Fig.12 Battery Power

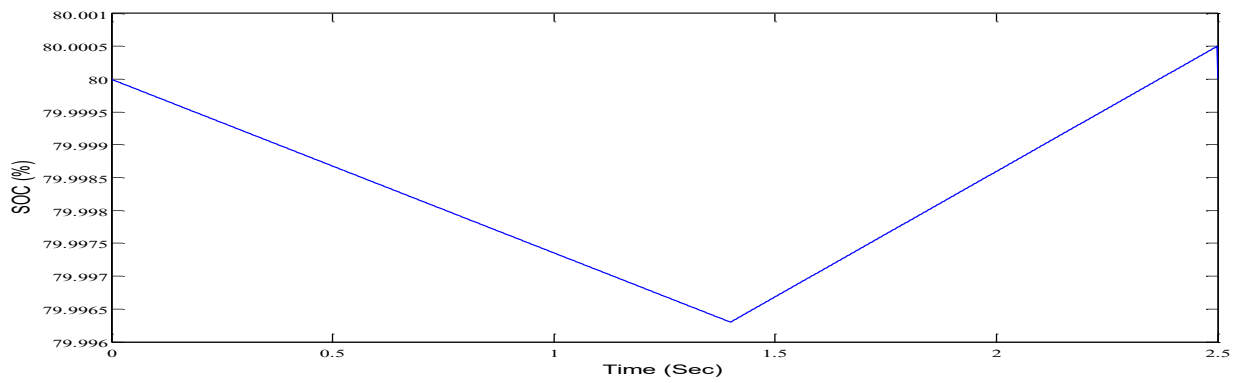


Fig.13 SOC

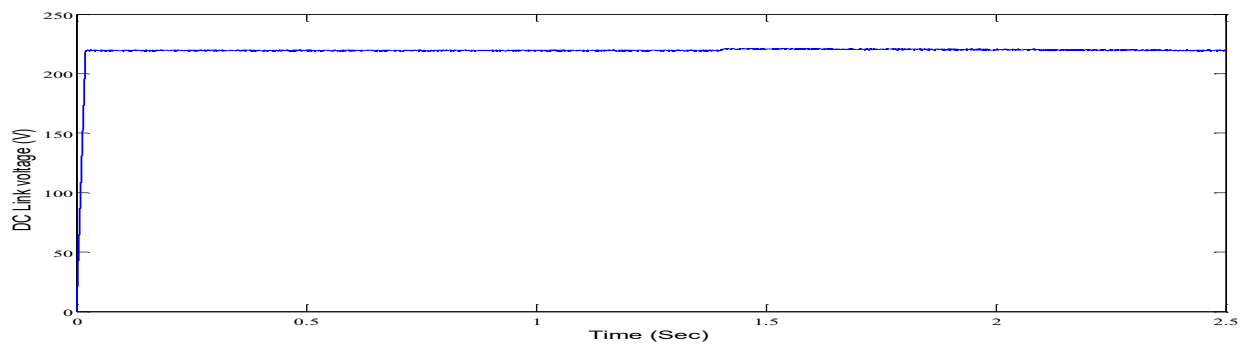


Fig.14 DC Link voltage

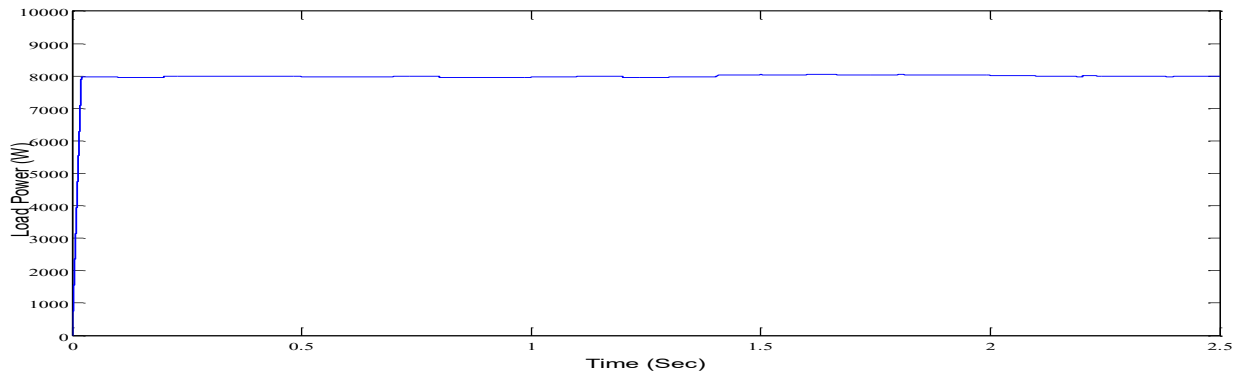


Fig.15 Load Power

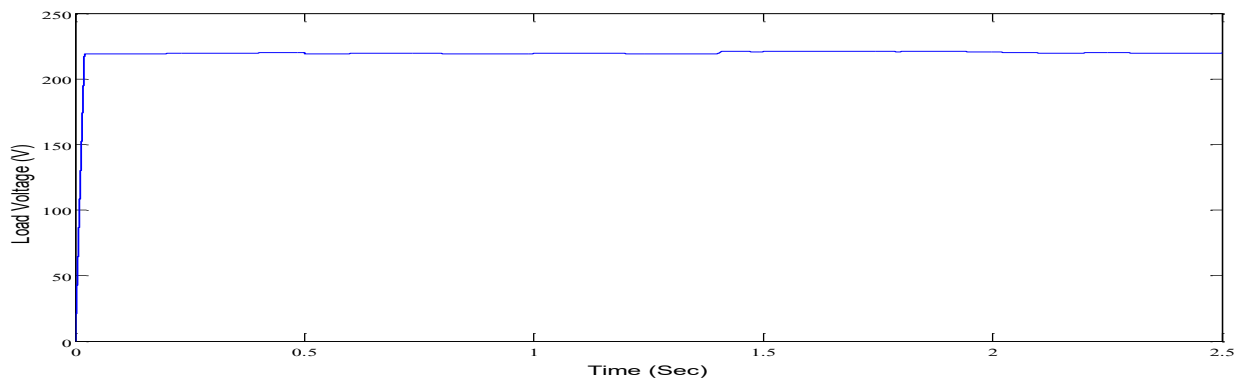


Fig.16 Load Voltage

In Figs. 17 and 18, we simulate a random fluctuation in wind speed and solar radiation to test the proposed energy management strategy. Fig. 19 shows the wind power output under varying wind conditions. This discussion suggests that the wind system could be used for maximum power point tracking (MPPT). Maximum power point tracking (MPPT) control, as shown in Figure 20, keeps the PV panel operating at peak efficiency.

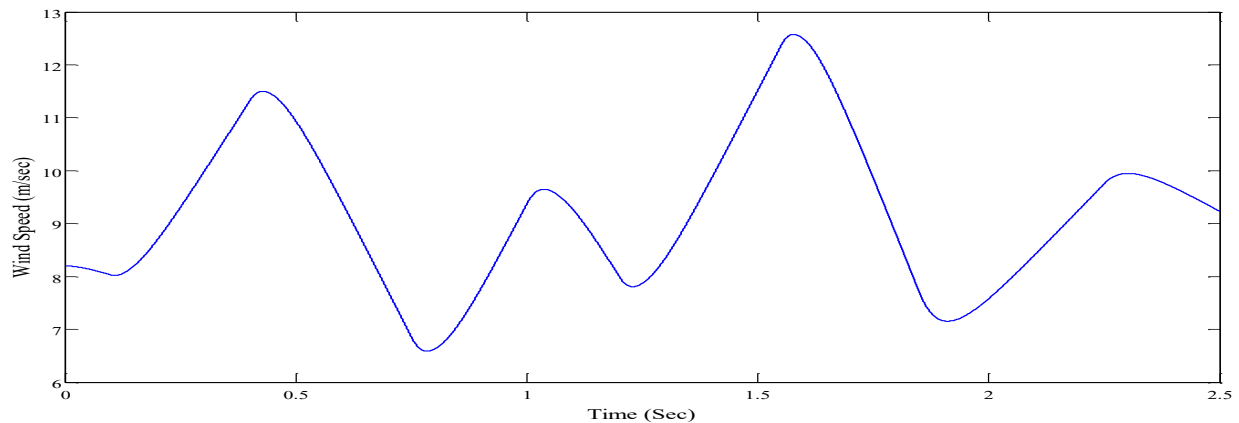


Fig.17 Wind Speed

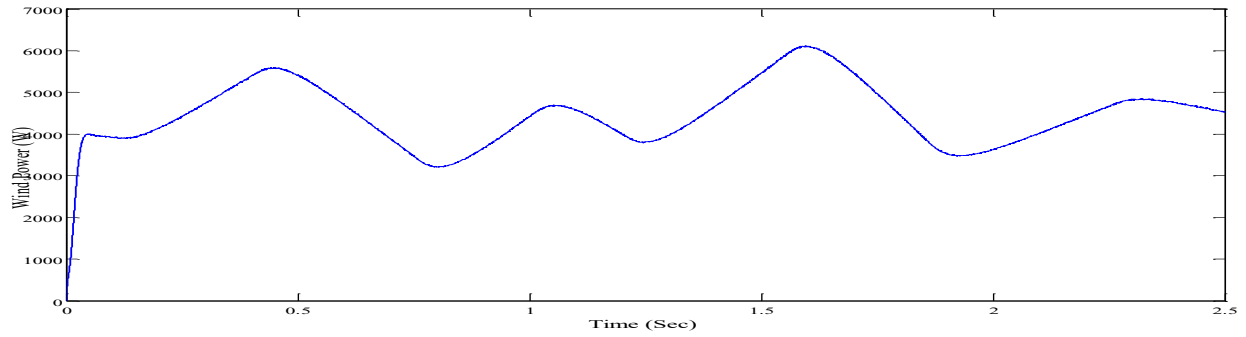


Fig.18 Wind Power

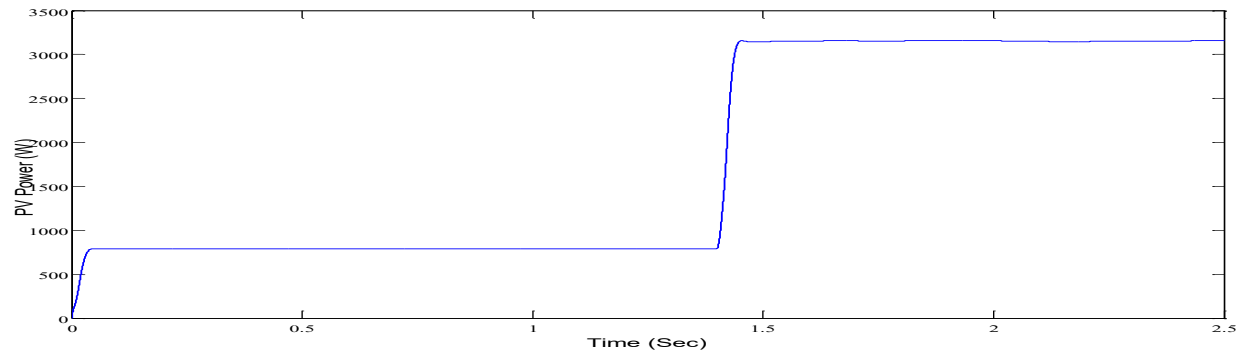


Fig.19 PV Power

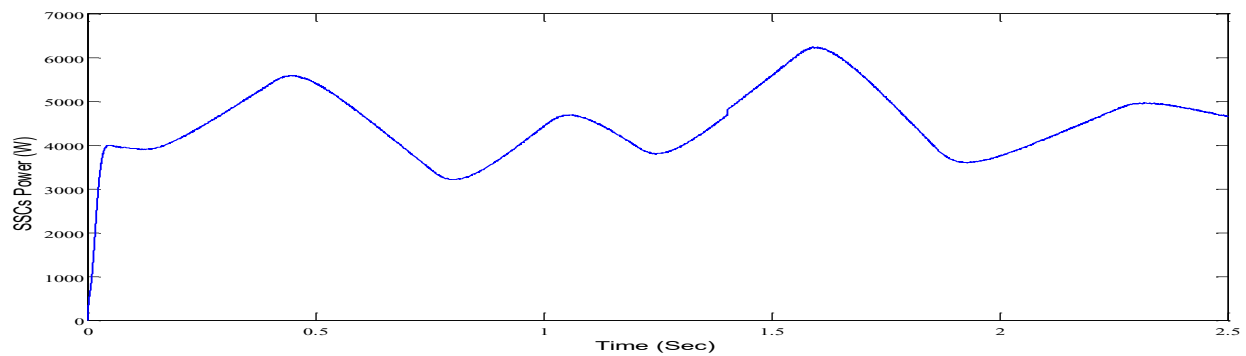


Fig.20 SSCs Power

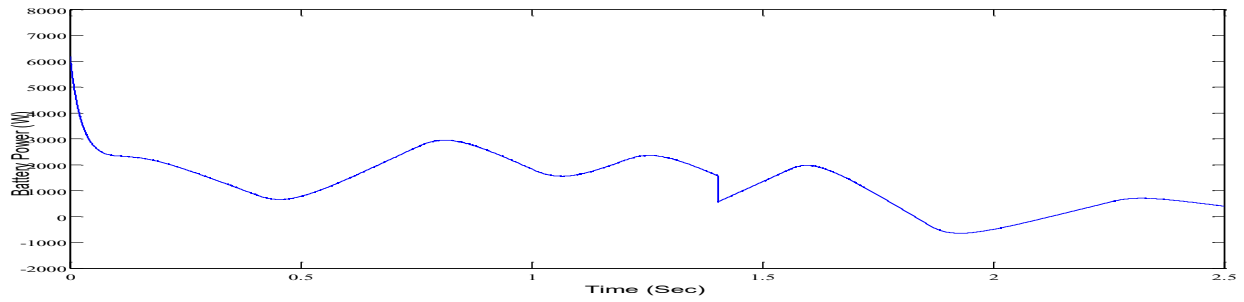


Fig.21 Battery Power

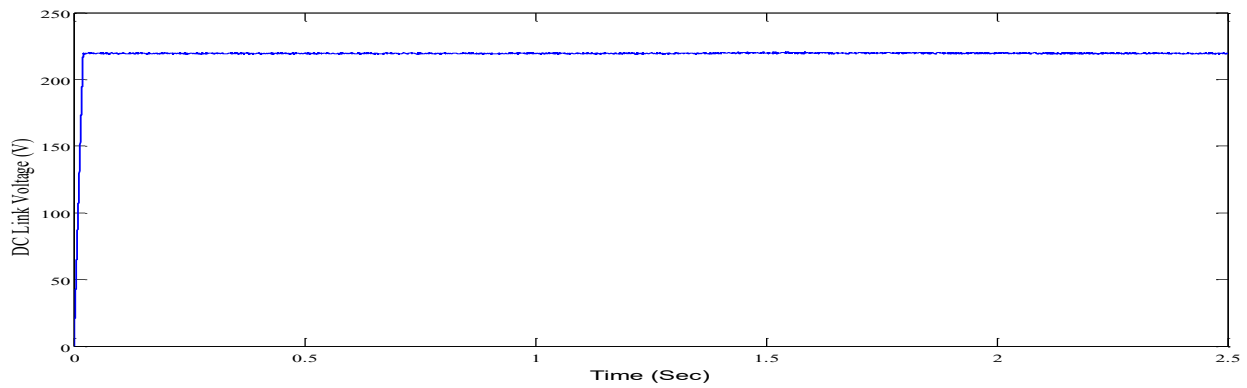


Fig.22 DC Link Voltage

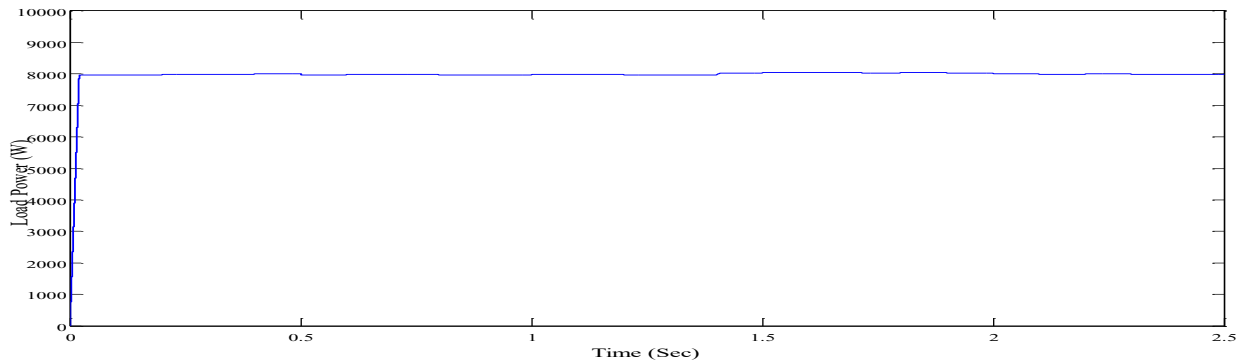


Fig.23 Load Power

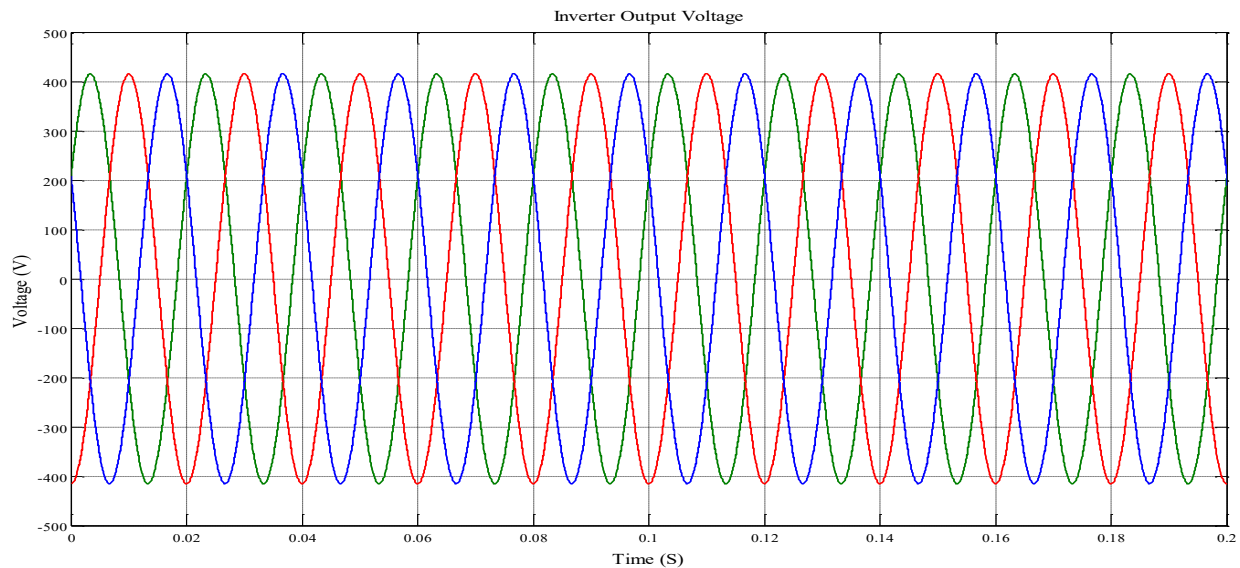


Fig. 24 Inverter output voltage with filter

4 Conclusion

In order to develop and operate an independent micro-grid, this study suggests using a PV system and a WECS. The PV system's power collection was optimised and regulated using a boost converter that uses ANN MPPT. The output of the PV system was controlled by two PI voltage and current loops, which ensured that the voltage through the DC bus for the battery bank remained constant. We made sure the control system would work reliably no matter what. When the amount of energy generated by the PV panels exceeds what the load needs, the batteries are charged. Discharging the batteries provides a boost in power when the energy provided by the PV modules is insufficient. In addition, a controller prevents the battery banks from being subjected to normal, overcharging, or overdischarging conditions. In any given situation, the controller must take the appropriate action. The controller will work properly with a battery charge of 20% to 80%. The PV panels and wind turbine are instructed to turn off when the SOC falls below 80%. Until the SOC drops below a preset threshold typically 75% this controller will prevent the PV panels and wind turbine from connecting. Extra instructions to switch off the inverter and unplug the loads are sent out when the state of charge falls below 20%. Once the batteries are dead, the inverter won't get any juice. Now that the autonomous system is up and running

References

1. Bendary, A.F.; Ismail, M.M. Battery charge management for hybrid PV/wind/fuel cell with storage battery. *Energy Procedia* 2019, 162, 107–116. [CrossRef]



2. Elavarasan, R.M.; Ghosh, A.; Mallick, T.K.; Krishnamurthy, A.; Saravanan, M. Investigations on performance enhancement measures of the bidirectional converter in PV–wind interconnected microgrid system. *Energies* 2019, 12, 2672. [CrossRef]
3. Muriithi, G.; Chowdhury, S. Optimal energy management of a grid-tied solar PV-battery microgrid: A Reinforcement learning approach. *Energies* 2021, 14, 2700. [CrossRef]
4. Shan, Y.; Hu, J.; Chan, K.W.; Fu, Q.; Guerrero, J.M. Model predictive control of bidirectional DC-DC converters and AC/DC interlinking converters—A new control method for PV-wind-battery microgrids. *IEEE Trans. Sustain. Energy* 2019, 10, 1823–1833. [CrossRef]
5. Mahesh, A.; Sandhu, K.S. Hybrid wind/photovoltaic energy system developments: Critical review and findings. *Renew. Sustain. Energy Rev.* 2015, 52, 1135–1147. [CrossRef]
6. Berardi, U.; Tomassoni, E.; Khaled, K. A smart hybrid energy system grid for energy efficiency in remote areas for the army. *Energies* 2020, 13, 2279. [CrossRef]
7. Murty, V.V.S.N.; Kumar, A. Multi-objective energy management in microgrids with hybrid energy sources and battery energy storage systems. *Prot. Control Mod. Power Syst.* 2020, 5, 1–20. [CrossRef]
8. Alhasnawi, B.N.; Jasim, B.H.; Esteban, M.D. A new robust energy management and control strategy for a hybrid microgrid system based on green energy. *Sustainability* 2020, 12, 5724. [CrossRef]
9. Kumar, G.R.P.; Sattianadan, D.; Vijayakumar, K. A survey on power management strategies of hybrid energy systems in microgrid. *Int. J. Electr. Comput. Eng. IJECE* 2020, 10, 1667–1673. [CrossRef]
10. Datta, U.; Kalam, A.; Shi, J. Hybrid PV–wind renewable energy sources for microgrid application: An overview. In *HybridRenewable Energy Systems in Microgrids*; Elsevier BV: Amsterdam, The Netherlands, 2018; pp. 1–22.
11. Rehman, S.; Habib, H.U.R.; Wang, S.; Buker, M.S.; Alhems, L.M.; Al Garni, H.Z. Optimal design and model predictive control of standalone HRES: A real case study for residential demand side management. *IEEE Access* 2020, 8, 29767–29814. [CrossRef]
12. Fathy, A.; Kaaniche, K.; Alanazi, T.M. Recent approach Based social spider optimizer for optimal sizing of hybrid PV/wind/battery/diesel integrated microgrid in Aljouf region. *IEEE Access* 2020, 8, 57630–57645. [CrossRef]
13. Luo, Y.; Yang, D.; Yin, Z.; Zhou, B.; Sun, Q. Optimal configuration of hybrid-energy microgrid considering the correlation and randomness of the wind power and photovoltaic power. *IET Renew. Power Gener.* 2020, 14, 616–627. [CrossRef]
14. Yahaya, A.A.; Al-Muhaini, M.; Heydt, G.T. Optimal design of hybrid DG systems for microgrid reliability enhancement. *IET Gener. Transm. Distrib.* 2020, 14, 816–823. [CrossRef]
15. Samy, M.; Mosaad, M.I.; Barakat, S. Optimal economic study of hybrid PV-wind-fuel cell system integrated to unreliable electric utility using hybrid search optimization technique. *Int. J. Hydrog. Energy* 2021, 46, 11217–11231. [CrossRef]
16. Lamichhane, A.; Zhou, L.; Yao, G.; Luqman, M. LCL Filter based grid-connected photovoltaic system with battery energy storage. In *Proceedings of the 2019 14th IEEE Conference on Industrial Electronics and Applications (ICIEA), Xi'an, China, 19–21 June 2019*; Institute of Electrical and Electronics Engineers (IEEE): New York, NY, USA, 2019; pp. 1569–1574.



17. 1STH-215-P Solar Panel from 1Soltech Specifications. Available online: http://www.posharp.com/1sth-215-p-solar-panel-from_1soltech_p1621902445d.aspx (accessed on 25 July 2021).
18. Al-Mahmodi, M.; Al-Quraan, A. On-grid solar energy system—A study case in Irbid. In Proceedings of the 6th Global Conference on Renewable Energy and Energy Efficiency for Desert Regions (GCREEDER 2018), Amman, Jordan, 3–5 April 2018.
19. Rathore, A.; Patidar, N. Reliability assessment using probabilistic modelling of pumped storage hydro plant with PV-wind based standalone microgrid. *Int. J. Electr. Power Energy Syst.* 2019, 106, 17–32. [CrossRef]
20. Al-Quraan, A.; Stathopoulos, T.; Pillay, P. Comparison of wind tunnel and on site measurements for urban wind energy estimation of potential yield. *J. Wind. Eng. Ind. Aerodyn.* 2016, 158, 1–10. [CrossRef].
21. Stathopoulos, T.; Alrawashdeh, H.; Al-Quraan, A.; Blocken, B.; Dilimulati, A.; Paraschivoiu, M.; Pilay, P. Urban wind energy: Some views on potential and challenges. *J. Wind Eng. Ind. Aerodyn.* 2018, 179, 146–157. [CrossRef]
22. Yang, D.; Jiang, C.; Cai, G.; Huang, N. Optimal sizing of a wind/solar/battery/diesel hybrid microgrid based on typical scenarios considering meteorological variability. *IET Renew. Power Gener.* 2019, 13, 1446–1455. [CrossRef]